Geophysical Research Letters

Key Points:
- We provide the first global nonstationary assessment of changes in the magnitude, return period, and probability of observed extreme floods
- We find increasing 20-year and 50-year floods in temperate climate zones but mostly decreases in arid, tropical, polar, and cold zones
- For the 100-year floods, at a smaller sample of sites, we find decreases in arid and temperate zones and mixed results elsewhere

Supporting Information:
- Supporting Information S1

Correspondence to:
L. Slater,
louise.slater@ouce.ox.ac.uk

Global Changes in 20-Year, 50-Year, and 100-Year River Floods

L. Slater[1] , **G. Villarini[2]** , **S. Archfield[3]** , **D. Faulkner[4]** , **R. Lamb[5,6]** , **A. Khouakhi[7]** , and **J. Yin[8]**

[1]School of Geography and the Environment, University of Oxford, Oxford, UK, [2]IIHR - Hydroscience & Engineering, University of Iowa, Iowa City, IA, USA, [3]U.S. Geological Survey, Reston, VA, USA, [4]JBA Consulting, Skipton, UK, [5]JBA Trust, Skipton, UK, [6]Lancaster Environment Centre, Lancaster University, Lancaster, UK, [7]School of Water, Energy and Environment, Center for Environmental and Agricultural Informatics, Cranfield University, Cranfield, UK, [8]State Key Laboratory of Water Resources and Hydropower Engineering Science, Wuhan University, Wuhan, China

Abstract Concepts like the 100-year flood event can be misleading if they are not updated to reflect significant changes over time. Here, we model observed annual maximum daily streamflow using a nonstationary approach to provide the first global picture of changes in: (a) the magnitudes of the 20-, 50-, and 100-year floods (i.e., *flows of a given exceedance probability in each year*); (b) the return periods of the 20-, 50-, and 100-year floods, as assessed in 1970 (i.e., *flows of a fixed magnitude*); and (c) corresponding flood probabilities. Empirically, we find the 20-/50-year floods have mostly increased in temperate climate zones, but decreased in arid, tropical, polar, and cold zones. In contrast, 100-year floods have mostly decreased in arid/temperate zones and exhibit mixed trends in cold zones, but results are influenced by the small number of stations with long records, and highlight the need for continued updating of hazard assessments.

Plain Language Summary Here, we provide the first global examination of recent changes in the size, frequency, and probability of extreme river floods using historical river records. Since the 1970s, the 20-year and 50-year extreme river floods have mostly increased in temperate zones but decreased in arid, tropical, polar, and cold zones. In contrast, the 100-year floods have decreased in arid and temperate zones, and show mixed results in cold zones, but at a smaller sample of sites with long records. Descriptions of changes in extreme flooding depend largely on site selection, and are constrained by availability of long-term data. Overall, our findings highlight the importance of regularly updating flood hazard assessments under nonstationarity.

1. Introduction

Return periods like the "*T*-year (100-year) event" describe an environmental event that has, on average, a 1-in-*T* (1% for the 100-year event) chance of occurring or being exceeded in any given year, at a given location. However, there is consensus that the frequency and magnitude of extremes such as floods are changing dynamically with shifts in climate (Hirabayashi et al., 2013; Hoegh-Guldberg et al., 2018), land cover (Blum et al., 2020; Vogel et al., 2011), or both (Yin et al., 2018). As a result, many people have questioned the validity of assuming time-invariant probability distributions to estimate risk—such as the risk of flooding (Milly et al., 2008; Read & Vogel, 2015; Salas & Obeysekera, 2019; Yan et al., 2017). There is growing acceptance that stationary concepts like a fixed 1-in-100-year flood are too easily misinterpreted (HM Government, 2016) and new methods are required to better represent time-varying probability distributions reflecting the ubiquity of global changes in climate and land cover (see e.g., Slater et al. [2020] for a review).

Nonstationary methods are widely used to estimate changes in the properties of extremes—such as the magnitude, frequency, duration, variability, or timing of flooding (Archfield et al., 2016; Eastoe, 2019; Hecht & Vogel, 2020; Salas & Obeysekera, 2019; Slater & Villarini, 2016; Villarini, Serinaldi, Smith, & Krajewski, 2009). The advantage of these approaches is their ability to model changes in the distribution of extreme events as a function of explanatory variables such as time, indices representing climate variability (e.g., Silva et al., 2016; Steirou et al., 2019), or land cover (Prosdocimi et al., 2015; Villarini et al., 2009). Various distributions (such as the Generalized Extreme Value or log Pearson type-III distributions) have been

used to estimate changes in the magnitude of extremes, such as the annual/seasonal series of maximum streamflow (Faulkner, Warren, Spencer, & Sharkey, 2020; Prosdocimi et al., 2015). In contrast, the GAMLSS framework (Generalized additive models for location, scale, and shape) has the advantage of being able to fit a broad range of distributions to the response variable, and allows the distribution parameters to be modeled as linear or smooth functions of explanatory variables (Rigby et al., 2019). GAMLSS models are a popular alternative for explaining changes in design floods (e.g., Yan et al., 2017), flood flashiness (Saharia et al., 2017), and flood magnitudes as a function of explanatory variables such as time, urbanization (e.g., Villarini et al., 2009), or even reservoir indices (López & Francés, 2013).

Application of nonstationary methods is beginning to extend beyond research settings and become adopted by environmental management authorities, for instance in the design of flood mitigation schemes (European Cooperation in Science and Technology, 2013; Faulkner et al., 2020). A range of technical approaches has been proposed to improve flood risk management, including the design of engineering structures such as dikes, dams, sewers or bridges. These include evaluating time-evolving changes in: the return period or "expected waiting time" (EWT) of an event (Luke et al., 2017; Obeysekera & Salas, 2016; Salas & Obeysekera, 2019; Salas et al., 2018); the return period of the stationary 100-year event (Villarini et al., 2009); the design life level (DLL) of structures (Rootzén & Katz, 2013); the short-term risk (Towe et al., 2020); the expected number of exceedances or equivalent reliability of an event (Yan et al., 2017). However, there has not yet been a global empirical assessment of nonstationarity in different flood extremes and how it differs across climate regions.

Here, we provide the first global examination of changes in the return periods and probabilities of observed extreme peak river flows and a discussion of the sensitivity of the results to different approaches, including site selection. We use a nonstationary distributional regression (Stasinopoulos et al., 2018) approach— sometimes referred to as a time-varying moments model (Zhang et al., 2018)—where the series' distribution parameters are expressed as functions of time. We: (1) quantify how the magnitudes of flows of a given exceedance probability (e.g., 20-, 50-, and 100-year return period) have changed over the historical record in each stream gauge; (2) estimate how the return periods of flows of given magnitude (e.g., 20-, 50-, and 100-year flood as assessed in the 1970s) have changed over time, from the 1970s to today; and (3) assess corresponding changes in flood probabilities. We visualize these changes, describe the uncertainties involved, and discuss the advantages and drawbacks of different nonstationary measures for describing changes in extreme floods.

2. Data and Methods

We obtained 10,093 river gauge records from a combination of global and national streamflow archives extending from before 1980 to after 2007 (see Methods in the supporting information for full details and filtering criteria; Figure S1 for entire record length; recent data extend to 2019). The 1970s are selected as a reference point to compare changes in flood return periods because this decade provides a good compromise for observed streamflow record length and availability worldwide. All stream gauges are used, not only those in benchmark or near natural conditions, to obtain a realistic picture of changing flood hazard, whether "natural" or modified by anthropogenic influences like flood defences. The entire record length is employed at each site to reduce uncertainties in the detection of changes in extremes. We require a strict minimum of 30, 50, and 70 complete years of data to estimate changes in the 20-, 50-, and 100-year return periods, respectively. These selected record lengths represent a trade-off between statistical requirements for robustness (ideally, the record length should exceed the magnitude of the extreme under consideration) and global data availability (few countries actually have observed flow records longer than a few decades). Stations with insufficient record length are dropped from the analysis (e.g., if a site has a 30-year record, we only compute changes in the 20-year flood but not changes in 50- or 100-year return periods). Increasing the record length requirement for extremes is technically more robust and allows us to assess consistency in the magnitude and direction of changes in 20-, 50-, and 100-year extremes when using fewer sites with long records.

At each site, we fit both a stationary model (i.e., constant parameters) and nonstationary models (i.e., one or both parameters dependent on time), and select the best-fitting GAMLSS model (Table S1, Figure S2).
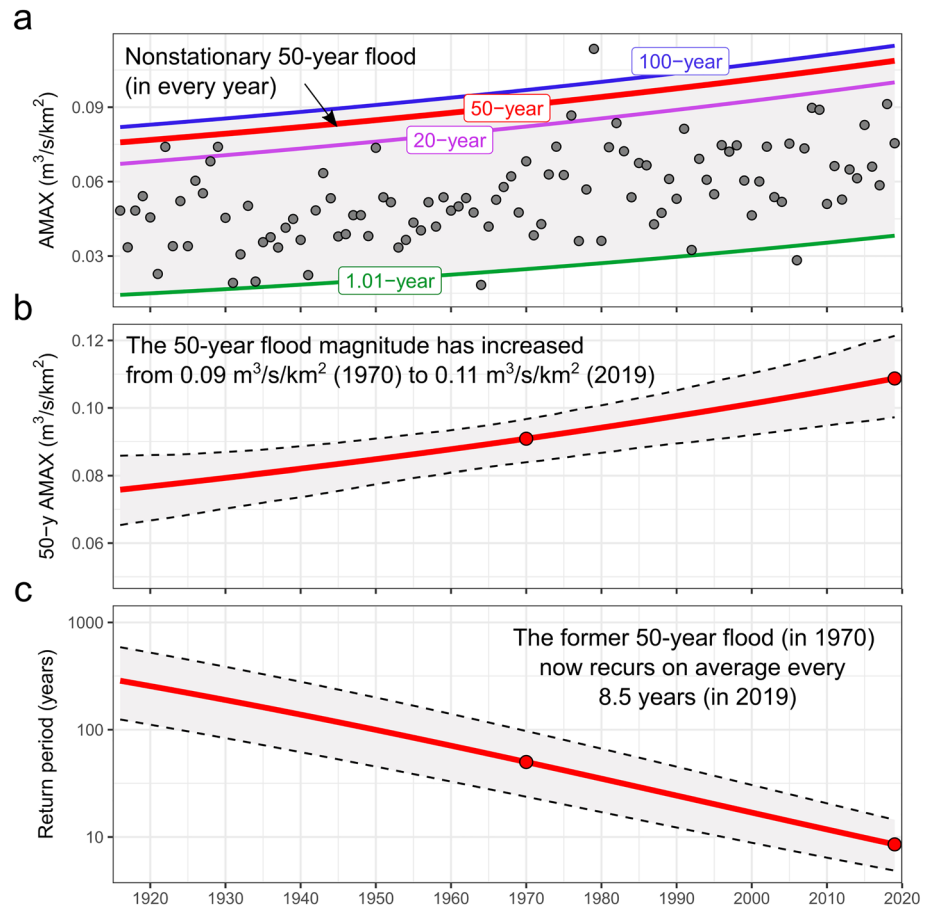
Figure 1. Example of changes in flood magnitude and return period at one site, the Kanakee River at Momence, Illinois (USA). (a) Black circles indicate observed time series of annual maximum daily flows from water years 1916–2019. Centile curves for the best-fitting nonstationary model (Gamma) indicate the estimated nonexceedance probabilities (1%, 95%, 98%, 99%) corresponding to the 1.01-, 20-, 50-, and 100-year flood return periods in each year (defined on the annual maximum scale). (b) We extract the 50-year flood estimated in every year (same as the red line in panel a) and add 5th and 95th percentile confidence intervals to these estimates as dashed lines. Red circles indicate the estimated 50-year flood in 1970 (0.09 m^3/s/km^2) and 2019 (0.11 m^3/s/km^2). (c) The return period of the 50-year flood estimated in 1970 (and its associated confidence intervals) is then estimated in every year using the time-varying model parameters. Red circles indicate the estimated return period in 1970 (50 years) and 2019 (8.5 years).

At sites where the nonstationary model indicates the best fit, that is, 35% of the 9350 sites where models could be fitted (Methods in the supporting information), we estimate year-to-year changes in magnitudes of the 20-, 50-, and 100-year floods (Figure 1a). We extract the value of the 20-, 50-, and 100-year flood in the 1970s (from a nonstationary model fitted to the whole record, setting the time covariate to the earliest water year available in the 1970s at each site), along with the corresponding confidence intervals (Figure 1b) to compute the changing return periods and uncertainties by today (where "today" means the most recent complete water year available since 2007; Figure 1c). The uncertainties tend to be smaller at sites with very long (e.g., >100-year) records, but otherwise vary considerably from site-to-site, irrespective of record length (Figure S3). Sites where the flood magnitude has decreased considerably over time tend to have the largest uncertainties in the recent period (Figure S4 and Methods in the supporting information).

3. Results and Discussion

3.1. Flood Magnitudes

The magnitudes of the 20-, 50-, and 100-year flood flows estimated using nonstationary models have both increased and decreased in different regions of the world since the 1970s (Figures 2 and S5). Grouping the
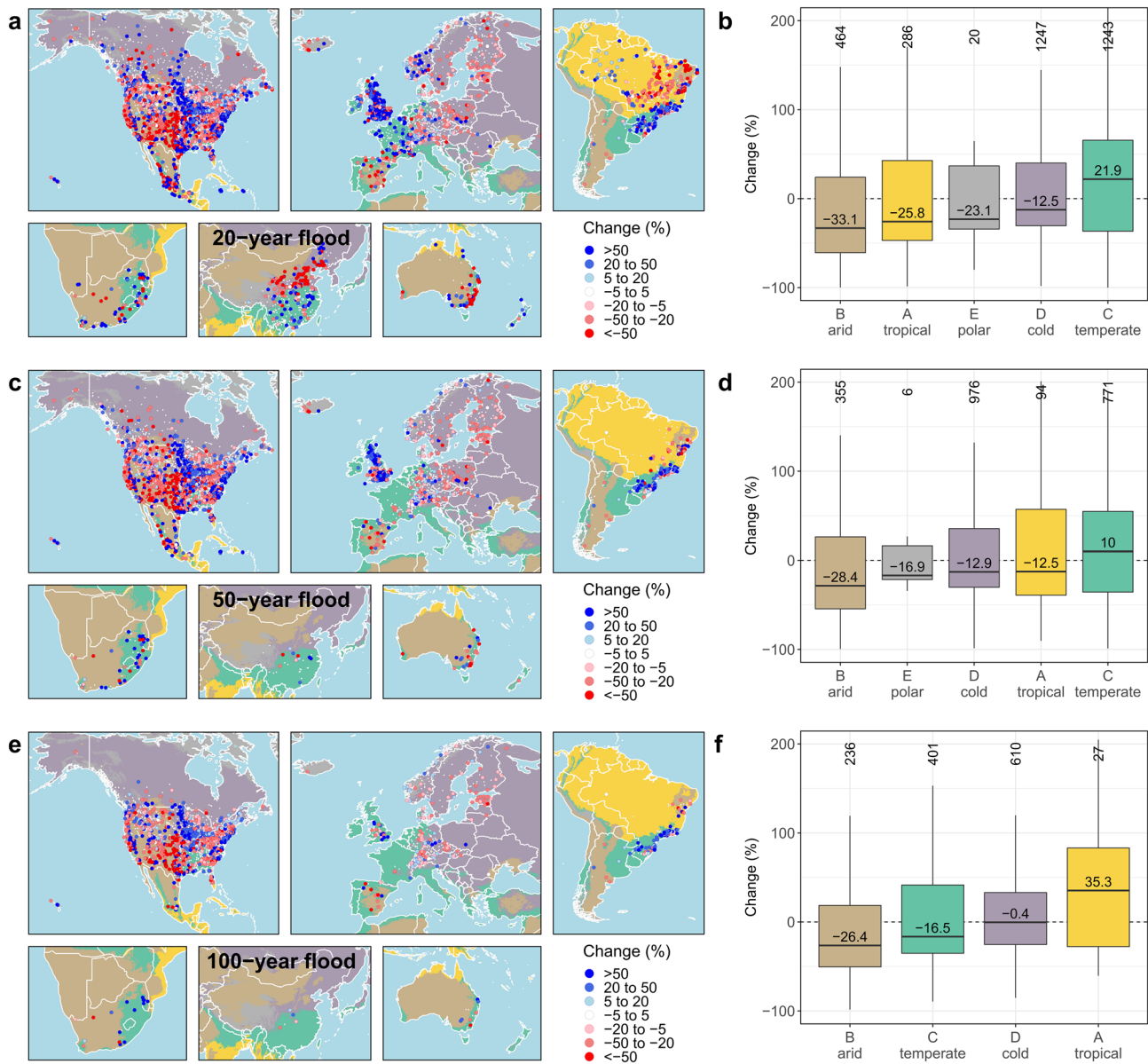
Figure 2. What is the change in the magnitude of the 20-, 50-, and 100-year floods since the 1970s? (a) and (b) Percent change in the magnitude of the 1970s-based 20-year flood today; (c) and (d) 50-year flood; (e)–(f) 100-year flood. Background shades indicate the 5 Köppen-Geiger climate regions (Beck et al., 2018): tropical, arid, temperate, cold, and polar. (a, c, e) Blue (red) circles indicate stream gauges where floods have increased (decreased) by more than 50%, 20%, and 5% relative to the *T*-year flood. Small white circles indicate sites with stationary records. Global maps are shown in Figure S5. (b, d, f) Boxplots indicate the distribution of change (%) for sites with nonstationary records in each Köppen-Geiger climate region (lower and upper hinges correspond to the first and third quartiles; whiskers extend to the smallest/largest value at most 1.5 times the interquartile range from the hinge). Median values are indicated horizontally; number of sites above each boxplot. Boxplot not shown for the polar region in panel (f) because $n = 1$.

sites by the five broad Köppen-Geiger climate regions (Beck et al., 2018), we find that estimates of change vary notably. The median change in the 20-year flood magnitude is +21.9% at 1243 sites in temperate regions (Figures 2a and F2b). Increases are particularly apparent in Atlantic Europe, southeastern Brazil, and southeastern China. In contrast, we find decreasing flood magnitudes, on average, in arid (median −33.1%); tropical (median −25.8%), polar (−23.1%) and cold (−12.5%) Köppen-Geiger regions. Decreases are most visible in northeastern Brazil, eastern Europe, parts of western USA, and parts of northern China. The African continent has very few publicly accessible streamflow data records, but a recent database suggests that floods have mostly been increasing in western and southern Africa since the 1980s (Tramblay et al., 2020). These spatial patterns of change are distinct but far from homogeneous: many regions exhibit a mix of sites

with increasing and decreasing flood magnitudes. Some of the flood decreases may be caused by decreasing soil moisture, where drier antecedent conditions offset flood magnitudes (Slater & Villarini, 2016; Wasko & Nathan, 2019), possibly due to increasing temperatures (e.g., eastern Europe, western USA), negative rainfall trends (e.g., eastern Australia), or groundwater depletion (e.g., Southern California, North China Plain [Rodell et al., 2018]).

Estimates of change depend on the observational data used to assess each flood extreme (the number of available sites decreases as the record length requirement increases). If the same sites were employed, then results would be relatively consistent across all extremes (20-/50-/100-year floods). However, as we restrict detection of changes in 50-/100-year floods to increasingly small site samples with long records, the average trends expressed for different climate zones may vary (e.g., Figures 2b vs. 2f). In arid and polar regions, flood magnitudes are decreasing on average for all three extremes: 20-, 50-, and 100-year floods (Figures 2b, 2d, and 2f). In tropical and cold regions, we find a majority of decreasing 20-/50-year floods, but different patterns for the 100-year flood. Conversely, in the temperate regions, we find a majority of increasing 20-/50-year floods, but decreasing 100-year floods (e.g., the UK). These differences are not surprising and depend on the smaller numbers of sites used to evaluate increasingly rare extremes.

Evidently, at each individual site, the direction and magnitude of change depend inherently on the choice of beginning and end dates (Harrigan et al., 2018) as well as the dominant flood-generating mechanisms and human influences. Changes in extreme floods are likely to be driven by a combination of climatic changes, land cover changes such as urbanization (e.g., Blum et al., 2020; Prosdocimi et al., 2015), agriculture, and anthropogenic influences on river regimes. The next step of such an analysis, inevitably, would be to tease out the underlying causes of the nonstationarity seen in these data (Salas et al., 2018). However, a detailed analysis of the covariates driving these changes in extreme floods is beyond the scope of this work.

To date, there has been limited evaluation of changes in extreme flood properties across climate regions. An assessment of trends in the 30-year flood found overall increases in their frequency and magnitude over Europe and the USA, but weaker increases over Brazil and Australia (Berghuijs et al., 2017). Trends in annual maximum daily streamflow (as opposed to rarer extremes like the 20+-year flood) were found to be mostly decreasing over western North America, northeastern Brazil, and eastern Europe; but increasing over parts of western Europe, western Brazil and parts of eastern North America (Do et al., 2017). Another study of trends in the 90th percentile and annual maximum of daily streamflow over 1951–2010 (Gudmundsson et al., 2019) found increases over the central USA and northwestern Europe, but decreases over southern Australia, eastern Brazil and western north-America. In Australia, analysis of changes in the annual maximum flow (Ishak et al., 2013) found mostly decreases in floods along eastern and southeastern Australia, and some increases in the north. In China, significant decreases in flooding have been found over large parts of the Yellow River over 1990–2010 (Bai et al., 2016). Our work broadly supports results found for lower-magnitude floods, but also suggests that national/regional averages should be discussed with care when countries span multiple climatic zones (e.g., China, Brazil, and the USA).

3.2. Flood Return Periods

Following the assessment of changes in extreme peak river flow magnitudes, we also measure changes in return periods. There has not yet been an evaluation of changes in return periods of extreme floods at the global scale. Changes in return periods help communicate whether environmental extremes are occurring more or less frequently relative to any chosen point in the past. At each site, we estimate the magnitude of the 20-, 50-, and 100-year flood in the 1970s. Using the time-varying distribution parameters at each site (Table S1), we estimate the changing return period of the 1970s floods in every year (Figures 1c and 3).

Changes in flood return periods mirror the changes in flood magnitude and vary greatly around the world (Figures 3 and S6), but some distinct regional patterns can be seen. The 20-, 50-, and 100-year floods of the 1970s have become, on average, ~41-, 152-, and 358-year floods under present-day conditions (at 3174/2164/1262 sites with nonstationary records, respectively). These overall decreases in flood frequency at nonstationary sites may be due to a combination of flood control measures, climatic changes, and long-term water storage/antecedent conditions (Rodell et al., 2018; Sharma et al., 2018). However, this global average masks considerable spatial redistribution of flood hazard across climate zones (Figure 3). In
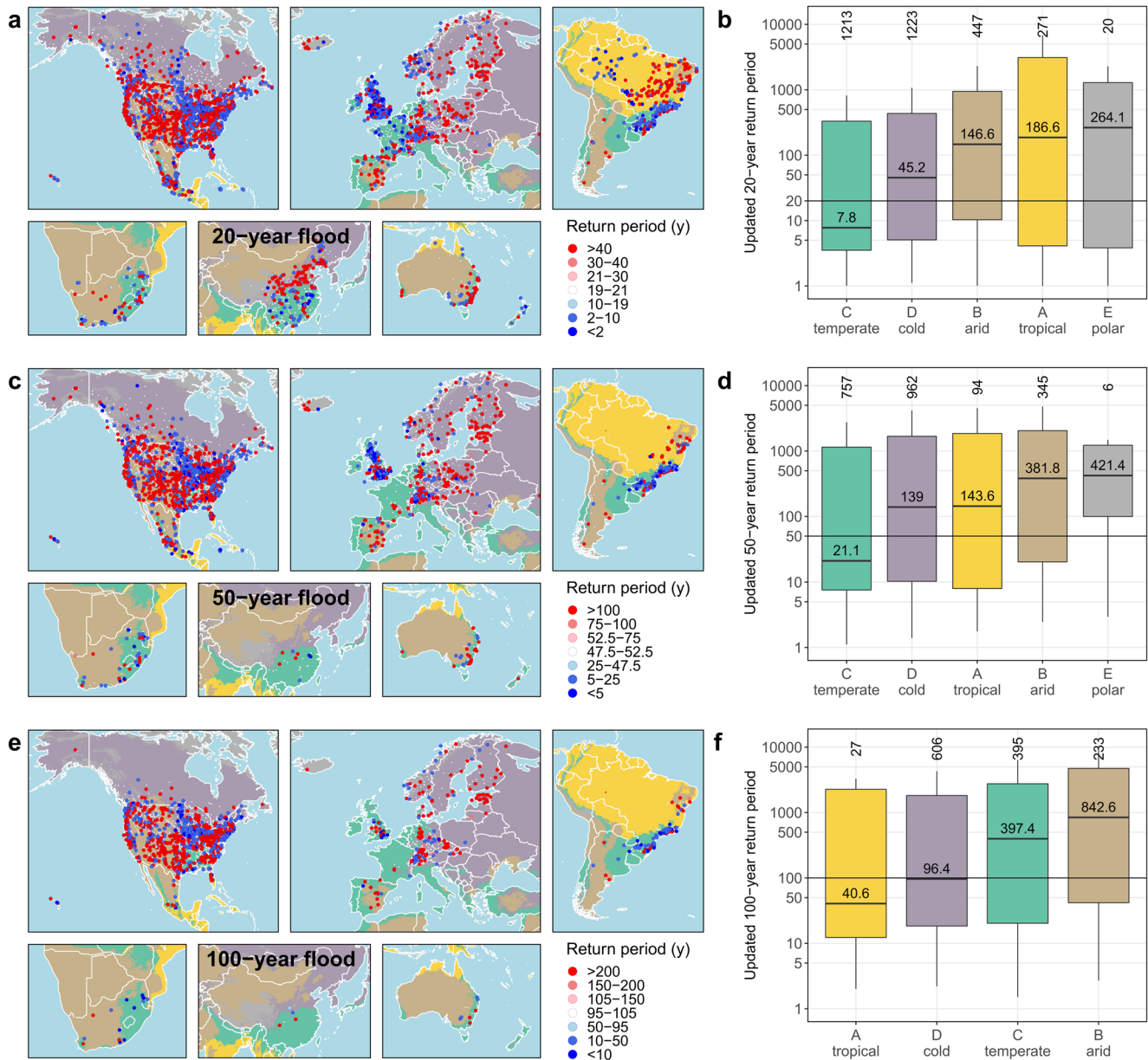
Figure 3. How have extreme flood return periods changed from the 1970s to today? (a, c, e) Present-day return period of the 20-, 50-, and 100-year flood as estimated in the 1970s (respectively). Red (blue) circles indicate increases (decreases) in return period since the 1970s. We only compute the evolving 20-/50-/100-year return periods at sites that have at least 30/50/70 years of complete data, respectively. Small white circles indicate sites with stationary records. Large circles indicate sites with greatest confidence, where the signs of the 5th and 95th percentile confidence intervals agree (Blöschl et al., 2019); smaller color circles (very few in number, e.g., one in western Brazil, panel e) indicate sites where signs do not agree. (b, d, f) Boxplot symbology same as Figure 2. The numbers of sites differ slightly from Figure 2 because changes in return periods could not be computed everywhere. Global maps are provided in Figure S6.

temperate zones, we find decreasing return periods (indicating increasing flood frequency): the 20-/50-year flood is now an 8-/21-year flood, on average. In contrast, a majority of increasing return periods (decreasing flood hazard) are found for the 20-/50-year flood in cold (45-/139-year), arid (147-/382-year), tropical (187-/144-year), and polar (264-/421-year) Köppen-Geiger regions. Differences across extremes again indicate that the choice and availability of sites is a key factor when evaluating change. For instance, for the tropical zone, a substantial increase is found, on average, for the 20-year return period (271 sites) but a decrease, on average, for the 100-year return period (only 27 sites). Thus, caution should be employed when describing regional patterns of change. The new return periods should be seen as indicative of the general direction of

change rather than precise estimates, since averages depend on site selection, and more information may be available locally than when using a global data set.

3.3. Flood Probabilities

One alternative way to communicate the flood hazard is to employ the concept of annual exceedance probability (AEP) instead—that is, the probability that a flow of a given magnitude will be exceeded in a given year. An annual flood probability conveys the same information as a return period, defined on the annual maximum scale (since it is merely the inverse of that return period), but it expresses the time scale explicitly. Arguably, probabilities simplify expressions of change: for example—"our chance of being flooded this year is 10%, up from 1% in the past." As a result, some institutions such as the Environment Agency in England and the U.S. Geological Survey (USGS) have moved toward expressing extremes in terms of annual probabilities instead of return periods (Fleming, 2002; Holmes & Dinicola, 2010). However, event probabilities are equally likely to be flawed if they are not updated, and perhaps more important than choosing between the two, is using recent statistics that more realistically reflect the true hazard.

To illustrate changing AEPs, we compute an "updated stationary" assessment (e.g., Luke et al., 2017), which describes how the probability of exceeding a given flow during a planning horizon varies over time. We estimate the exceedance probability of the T-year flow representative of 1970 conditions over a fixed, 30-year period, which may be relevant for a mortgage (Read & Vogel, 2015) or infrastructure design horizon (Olsen, 2015). We then compute the updated 30-year exceedance probability estimate representative of recent conditions, using the same flow rate but an updated annual probability. The 30-year exceedance probability is $1-(1-p)^{30}$, where p is the fixed annual probability over the 30-year period.

At the global scale, consistent with results for flood magnitude and return periods, we find a decrease in flood probabilities, which contrasts with global increases in the frequency of extreme precipitation (Papalexiou & Montanari, 2019). The 20-year flood representative of conditions in 1970, which had a 79% chance of occurring over a 30-year horizon under conditions equivalent to the 1970s, now has a 52% chance of occurring (median of 3174 sites). The 50-year flood, which had a 45% chance of occurring over a 30-year horizon under conditions equivalent to the 1970s, now has an 18% chance of occurring (median of 2164 sites). Similarly, the 100-year flood, which had a 26% chance of occurring, now has an 8% chance of occurring (median of 1262 sites), based on an updated, but constant 30-year annual event probability over the lifetime of a 30-year mortgage or design horizon. For comparison with the analysis of return periods, we provide maps of these updated event probabilities in Figure S7.

4. Conclusions

Here, we provide a global assessment of changes in the magnitude, return period, and probability of extreme river floods. For the 20- and 50-year return periods, we find a majority of increasing floods in temperate climate zones, but a majority of decreasing floods in arid, tropical, polar, and cold climate zones. For the 100-year return periods (a smaller sample of sites with at least 70 years of data), we obtain slightly different results, with decreases in arid and temperate zones; mixed trends in cold zones; and increases at a small sample of tropical sites. These differences serve as a reminder that the regional results of nonstationary analyses depend inherently on site selection and different return periods (flood quantiles) of interest.

This work does not evaluate the flood drivers that led to regional patterns of change, whether tied to climate or land use change. Additional analyses could classify the sites by their catchment characteristics (climate, land cover, or reservoir storage) and use physically based covariates such as time series of the percent land cover (Blum et al., 2020; Prosdocimi et al., 2015), or climate and reservoir indices (López & Francés, 2013). Extrapolation of flood probability estimates into the future also requires knowledge of the causes of the change. One growing avenue is to bridge the gap between statistical modeling of past trends and physics-based modeling of future changes in the event-generating mechanisms using hybrid dynamical-statistical models (Slater & Villarini, 2018; Vecchi et al., 2011; Wang et al., 2009) and machine learning. Such approaches take advantage of the ability of physical models to predict and explain large-scale phenomena

and the strengths of the nonstationary statistical models to estimate probabilities of extreme events conditioned on observed data.

Overall, distributional regression models provide a convenient approach to detect changes in the magnitudes, return periods, and probabilities of extremes. However, such results, and their uncertainties, should always be treated with care. Our findings indicate that in presence of nonstationarity, local flood hazard assessments should be updated regularly (Luke et al., 2017; Towe et al., 2020), for example, in the aftermath of significant floods, or at a fixed interval such as every five years (UK Cabinet Office, 2015), to ensure regular provision of the most up-to-date estimates of changing flood probabilities.

Conflict of Interest

The authors declare no conflicts of interest relevant to this study.

Data Availability Statement

The data are available from (1) the GRDC (https://www.bafg.de/GRDC/EN/Home/homepage_node.html); (2) the Spanish Ecological transition ministry (https://ceh.cedex.es/anuarioaforos/default.asp; no English link available); (3) the Brazilian National Water Agency (ANA; http://www.snirh.gov.br/hidroweb/apresentacao; no English link available) and Bruno Guimarães for his Python webscraping code "scraping-hidroweb" (available on GitHub; no alternative link); (4) the UKCEH (https://nrfa.ceh.ac.uk/); (5) the U.S. Geological Survey (https://waterdata.usgs.gov/nwis); (6) Environment and Climate Change Canada (ECCC) through the Water Survey of Canada (WSC; https://wateroffice.ec.gc.ca/search/historical_e.html); (7) the Mexican Comisión Nacional del Agua (CONAGUA; https://www.gob.mx/conagua/articulos/sistema-de-informacion-hidrologica-sih); (8) the Hydroinformatic Data Center managed by Ministry of Water Resources of China.

References

Archfield, S. A., Hirsch, R. M., Viglione, A., & Blöschl, G. (2016). Fragmented patterns of flood change across the United States. *Geophysical Research Letters*, *43*, 10232–10239. https://doi.org/10.1002/2016GL070590

Bai, P., Liu, X., Liang, K., & Liu, C. (2016). Investigation of changes in the annual maximum flood in the Yellow River basin, China. *Quaternary International*, *392*, 168–177. https://doi.org/10.1016/j.quaint.2015.04.053

Beck, H. E., Zimmermann, N. E., McVicar, T. R., Vergopolan, N., Berg, A., & Wood, E. F. (2018). Present and future Köppen-Geiger climate classification maps at 1-km resolution. *Scientific Data*, *5*, 1–12. https://doi.org/10.1038/sdata.2018.214

Berghuijs, W. R., Aalbers, E. E., Larsen, J. R., Trancoso, R., & Woods, R. A. (2017). Recent changes in extreme floods across multiple continents. *Environmental Research Letters*, *12*, 114035. https://doi.org/10.1088/1748-9326/aa8847

Blöschl, G., Hall, J., Viglione, A., Perdigão, R. A. P., Parajka, J., Merz, B., et al. (2019). Changing climate both increases and decreases European river floods. *Nature*, *573*(7772), 108–111. https://doi.org/10.1038/s41586-019-1495-6

Blum, A. G., Ferraro, P. J., Archfield, S. A., & Ryberg, K. R. (2020). Causal effect of impervious cover on annual flood magnitude for the United States. *Geophysical Research Letters*, *47*, e2019GL086480. https://doi.org/10.1029/2019gl086480

Do, H. X., Westra, S., & Leonard, M. (2017). A global-scale investigation of trends in annual maximum streamflow. *Journal of Hydrology*, *552*, 28–43. https://doi.org/10.1016/j.jhydrol.2017.06.015

Eastoe, E. F. (2019). Nonstationarity in peaks-over-threshold river flows: A regional random effects model. *Environmetrics*, *30*(5), 1–18. https://doi.org/10.1002/env.2560

European Cooperation in Science and Technology. (2013). *A review of applied methods in Europe for flood-frequency analysis in a changing environment. WG4: Flood frequency estimation methods and environmental change.* Retrieved from http://www.wmo.int/pages/prog/hwrp/publications/Floodfreq_report.pdf

Faulkner, D., Griffin, A., Hannaford, J., Sharkey, P., Warren, S., Shelton, K., et al. (2020). *Development of interim national guidance on non-stationary fluvial flood frequency estimation – science report. Environment Agency, FRS18087/IG/R1.* Retrieved from https://www.gov.uk/government/publications/development-of-interim-national-guidance-on-non-stationary-fluvial-flood-frequency-estimation

Faulkner, D., Warren, S., Spencer, P., & Sharkey, P. (2020). Can we still predict the future from the past? Implementing non-stationary flood frequency analysis in the UK. *Journal of Flood Risk Management*, *13*(1), 1–15. https://doi.org/10.1111/jfr3.12582

Fleming, G. (2002). Learning to live with rivers – The ICE's report to government. *Proceedings - Institution of Civil Engineers: Civil Engineering*, *150*(5), 15–21. https://doi.org/10.1680/cien.150.1.15.38541

Gudmundsson, L., Leonard, M., Do, H. X., Westra, S., & Seneviratne, S. I. (2019). Observed trends in global indicators of mean and extreme streamflow. *Geophysical Research Letters*, *46*, 756–766. https://doi.org/10.1029/2018GL079725

Harrigan, S., Hannaford, J., Muchan, K., & Marsh, T. J. (2018). Designation and trend analysis of the updated UK Benchmark Network of river flow stations: The UKBN2 dataset. *Hydrology Research*, *49*(2), 552–567. https://doi.org/10.2166/nh.2017.058

Hecht, J. S., & Vogel, R. M. (2020). Updating urban design floods for changes in central tendency and variability using regression. *Advances in Water Resources*, *136*, 103484. https://doi.org/10.1016/j.advwatres.2019.103484

Hirabayashi, Y., Mahendran, R., Koirala, S., Konoshima, L., Yamazaki, D., Watanabe, S., et al. (2013). Global flood risk under climate change. *Nature Climate Change*, *3*(6), 1–6. https://doi.org/10.1038/nclimate1911

HM Government. (2016). *National Flood Resilience Review (September)*. Retrieved from https://www.gov.uk/government/publications/national-flood-resilience-review

Hoegh-Guldberg, O., Jacob, D., Taylor, M., Bindi, S., Brown, I., Camilloni, A., et al. (2018). *Impacts of 1.5°C of global warming on natural and human systems*. In Global Warming of 1.5°C. An IPCC Special Report.

Holmes, R. R., & Dinicola, K. (2010). 100-Year flood – It's all about chance. U.S. Geological Survey General Information Product 106. Retrieved from http://pubs.usgs.gov/gip/106/

Ishak, E. H., Rahman, A., Westra, S., Sharma, A., & Kuczera, G. (2013). Evaluating the non-stationarity of Australian annual maximum flood. *Journal of Hydrology*, *494*, 134–145. https://doi.org/10.1016/j.jhydrol.2013.04.021

López, J., & Francés, F. (2013). Non-stationary flood frequency analysis in continental Spanish rivers, using climate and reservoir indices as external covariates. *Hydrology and Earth System Sciences*, *17*(8), 3189–3203. https://doi.org/10.5194/hess-17-3189-2013

Luke, A., Vrugt, J. A., AghaKouchak, A., Matthew, R., & Sanders, B. F. (2017). Predicting nonstationary flood frequencies: Evidence supports an updated stationarity thesis in the United States. *Water Resources Research*, *53*(7), 5469–5494. https://doi.org/10.1002/2016WR019676

Milly, P. C. D., Betancourt, J., Falkenmark, M., Hirsch, R. M., Kundzewicz, Z. W., Lettenmaier, D. P., & Stouffer, R. (2008). Stationarity is dead: Whither water management? *Science*, *319*(5863), 573–574. https://doi.org/10.1126/science.1151915

Obeysekera, J., & Salas, J. D. (2016). Frequency of recurrent extremes under nonstationarity. *Journal of Hydrologic Engineering*, *21*(5), 1–9. https://doi.org/10.1061/(ASCE)HE.1943-5584.0001339

Olsen, J. R. (Ed.). (2015). *Adapting infrastructure and civil engineering practice to a changing climate*. Reston, VA: American Society of Civil Engineers. https://doi.org/10.1061/9780784479193

Papalexiou, S. M., & Montanari, A. (2019). Global and regional increase of precipitation extremes under global warming. *Water Resources Research*, *55*(6), 4901–4914. https://doi.org/10.1029/2018WR024067

Prosdocimi, I., Kjeldsen, T. R., & Miller, J. D. (2015). Detection and attribution of urbanization effect on flood extremes using nonstationary flood-frequency models. *Water Resources Research*, *51*, 4244–4262. https://doi.org/10.1002/2015WR017065

Read, L. K., & Vogel, R. M. (2015). Reliability, return periods, and risk under nonstationarity. *Water Resources Research*, *51*, 6381–6398. https://doi.org/10.1002/2015WR017089

Rigby, R., Stasinopoulos, M., Heller, G., & De Bastiani, F. (2019). *Distributions for modelling location, scale and shape: Using GAMLSS in R*. CRC Press. Retrieved from http://www.gamlss.com/wp-content/uploads/2018/01/DistributionsForModellingLocationScaleandShape.pdf

Rodell, M., Famiglietti, J. S., Wiese, D. N., Reager, J. T., Beaudoing, H. K., Landerer, F. W., & Lo, M. H. (2018). Emerging trends in global freshwater availability. *Nature*, *557*(7707), 651–659.

Rootzén, H., & Katz, R. W. (2013). Design life level: Quantifying risk in a changing climate. *Water Resources Research*, *49*, 5964–5972. https://doi.org/10.1002/wrcr.20425

Saharia, M., Kirstetter, P.-E., Vergara, H., Gourley, J. J., Hong, Y., & Giroud, M. (2017). Mapping flash flood severity in the United States. *Journal of Hydrometeorology*, *18*(2), 397–411. https://doi.org/10.1175/jhm-d-16-0082.1

Salas, J. D., & Obeysekera, J. (2019). Probability distribution and risk of the first occurrence of k extreme hydrologic events. *Journal of Hydrologic Engineering*, *24*(10), 1–10. https://doi.org/10.1061/(ASCE)HE.1943-5584.0001809

Salas, J. D., Obeysekera, J., & Vogel, R. M. (2018). Techniques for assessing water infrastructure for nonstationary extreme events: A review. *Hydrological Sciences Journal*, *63*(3), 325–352. https://doi.org/10.1080/02626667.2018.1426858

Sharma, A., Wasko, C., & Lettenmaier, D. P. (2018). If precipitation extremes are increasing, why aren't floods? *Water Resources Research*, *54*, 8545–8551. https://doi.org/10.1029/2018WR023749

Silva, A. T., Naghettini, M., & Portela, M. M. (2016). On some aspects of peaks-over-threshold modeling of floods under nonstationarity using climate covariates. *Stochastic Environmental Research and Risk Assessment*, *30*(1), 207–224. https://doi.org/10.1007/s00477-015-1072-y

Slater, L. J., Anderson, B., Buechel, M., Dadson, S., Han, S., Harrigan, S., et al. (2020). Nonstationary weather and water extremes: A review of methods for their detection, attribution, and management. *Hydrology and Earth System Sciences Discussions*, *1–54*. https://doi.org/10.5194/hess-2020-576

Slater, L. J., & Villarini, G. (2016). Recent trends in U.S. flood risk. *Geophysical Research Letters*, *43*, 12428–12436. https://doi.org/10.1002/2016GL071199

Slater, L. J., & Villarini, G. (2018). Enhancing the predictability of seasonal streamflow with a statistical-dynamical approach. *Geophysical Research Letters*, *45*, 6504–6513. https://doi.org/10.1029/2018GL077945

Stasinopoulos, M. D., Rigby, R. A., & De Bastiani, F. (2018). GAMLSS: A distributional regression approach. *Statistical Modelling*, *18*(3–4), 248–273. https://doi.org/10.1177/1471082X18759144

Steirou, E., Gerlitz, L., Apel, H., Sun, X., & Merz, B. (2019). Climate influences on flood probabilities in Europe. *Hydrology and Earth System Sciences*, *23*, 1305–1322. https://doi.org/10.5194/hess-23-1305-2019

Towe, R., Tawn, J., Eastoe, E., & Lamb, R. (2020). Modelling the clustering of extreme events for short-term risk assessment. *Journal of Agricultural, Biological, and Environmental Statistics*, *25*(1), 32–53. https://doi.org/10.1007/s13253-019-00376-0

Tramblay, Y., Villarini, G., & Zhang, W. (2020). Observed changes in flood hazard in Africa. *Environmental Research Letters*, *15*, 1040b5. https://doi.org/10.1088/1748-9326/abb90b

UK Cabinet Office. (2015). *National Risk Register of Civil Emergencies: 2015 edition*. National Risk Register of Civil Emergencies.

Vecchi, G. A., Zhao, M., Wang, H., Villarini, G., Rosati, A., Kumar, A., et al. (2011). Statistical-dynamical predictions of seasonal North Atlantic hurricane activity. *Monthly Weather Review*, *139*(4), 1070–1082. https://doi.org/10.1175/2010MWR3499.1

Villarini, G., Serinaldi, F., Smith, J. A., & Krajewski, W. F. (2009). On the stationary of annual flood peaks in the continental United States during the 20th century. *Water Resources Research*, *45*(8), 1–17. https://doi.org/10.1029/2008WR007645

Villarini, G., Smith, J. A., Serinaldi, F., Bales, J., Bates, P. D., & Krajewski, W. F. (2009). Flood frequency analysis for nonstationary annual peak records in an urban drainage basin. *Advances in Water Resources*, *32*(8), 1255–1266. https://doi.org/10.1016/j.advwatres.2009.05.003

Vogel, R. M., Yaindl, C., & Walter, M. (2011). Nonstationarity: Flood magnification and recurrence reduction factors in the United States. *Journal of the American Water Resources Association*, *47*(3), 464–474. https://doi.org/10.1111/j.1752-1688.2011.00541.x

Wang, H., Schemm, J. K. E., Kumar, A., Wang, W., Long, L., Chelliah, M., et al. (2009). A statistical forecast model for Atlantic seasonal hurricane activity based on the NCEP dynamical seasonal forecast. *Journal of Climate*, *22*(17), 4481–4500. https://doi.org/10.1175/2009JCLI2753.1

Wasko, C., & Nathan, R. (2019). Influence of changes in rainfall and soil moisture on trends in flooding. *Journal of Hydrology*, *575*(May), 432–441. https://doi.org/10.1016/j.jhydrol.2019.05.054

Yan, L., Xiong, L., Guo, S., Xu, C. Y., Xia, J., & Du, T. (2017). Comparison of four nonstationary hydrologic design methods for changing environment. *Journal of Hydrology*, *551*, 132–150. https://doi.org/10.1016/j.jhydrol.2017.06.001

Yin, J., Gentine, P., Zhou, S., Sullivan, S. C., Wang, R., Zhang, Y., & Guo, S. (2018). Large increase in global storm runoff extremes driven by climate and anthropogenic changes. *Nature Communications*, *9*, 4389. https://doi.org/10.1038/s41467-018-06765-2

Zhang, T., Wang, Y., Wang, B., Tan, S., & Feng, P. (2018). Nonstationary flood frequency analysis using univariate and bivariate time-varying models based on GAMLSS. *Water*, *10*, 819. https://doi.org/10.3390/w10070819

References From the Supporting Information

Albers, S. (2017). tidyhydat: Extract and tidy Canadian hydrometric data. *The Journal of Open Source Software*, *2*(20), 511. https://doi.org/10.21105/joss.00511

GRDC. (2020). *Global daily streamflow data from the global runoff data center, 56068*. Koblenz, Germany. Retrieved from https://www.bafg.de/GRDC/EN/Home/homepage_node.html

Hirsch, R. M., & De Cicco, L. A. (2015). User guide to Exploration and Graphics for RivEr trends (EGRET) and dataRetrieval: R packages for hydrologic data (version 2.0, February 2015): U.S. Geological Survey Techniques and Methods. Book 4, chap. A10, 93 p. Retrieved from https://dx.doi.org/10.3133/tm4A10

Stasinopoulos, D. M., & Rigby, R. A. (2007). Generalized additive models for location scale and shape (GAMLSS) in R. *Journal of Statistical Software*, *23*(7), 1–46. https://doi.org/10.18637/jss.v023.i07

Vitolo, C., Fry, M., & Buytaert, W. (2016). rnrfa: An R package to Retrieve, Filter and Visualize Data from the UK National River Flow Archive. *R Journal*, *8*(2) 102–116.